IASTED-ISC'2003

A ROBUST FAULT TOLERANT CONTROL FRAMEWORK: APPLICATION TO A SOLAR POWER PLANT

A. Cardoso[1], P. Gil[1,2], J. Henriques[1], P. Carvalho[1], H. Duarte-Ramos[2], A. Dourado[1]
[1] CISUC-Informatics Engineering Department, University of Coimbra, Pólo II 3030-290 Coimbra
[2] Electrical Engineering Department, UNL, 2825-114 Monte de Caparica
Portugal

Abstract

A robust fault-tolerant control framework is proposed and applied to a Distributed Solar Collector field. The framework considers a model-based approach to estimate the system's state variables for supervision and fault diagnosis purposes and a model-based predictive control combined with a recurrent neural network. The supervisor system includes a fault detection filter to generate residual signals, which are used to isolate and identify the faults. The control system is based on a non-linear adaptive constrained model-based predictive control scheme with steady-state offset compensation. To assess the controller's robustness and fault tolerance, some faults on the actuator, sensors and system parameters were considered.

Key Words

Fault-tolerant control systems, fault diagnosis, model-based predictive control, online training, robustness.

1. Introduction

Growing demands on reliability and safety have increased the use of fault-tolerant control framework to design process control systems. A usual approach considers a fault diagnosis module, which includes the detection, isolation and identification actions, followed by the fault's accommodation. That module considers a model-based fault detection filter to generate residual signals in order to detect and isolate the faults. The early detection of faults (system malfunctions) combined with a fault-tolerant control strategy can help avoiding system shut-down, breakdown and even catastrophes involving human fatalities and material damage [1].

The model-based fault detection filter considers the analytical redundancy inherent in the dynamic relationships between inputs and outputs of a system.

Usually, a mathematical model is used to derive a residual quantity, which is supposed to be "small" for an unfaulty plant and "large" whenever a fault occurs. Faults could then be detected if the residual exceeds a given threshold. To achieve fault isolation, a set of residuals could be used, each one indicating a different fault. Surveys can be found for instance in [2], [3] and [4].

The fault detection filter is designed to generate a set of residuals corresponding to the expected faults in the system. The residual signals can be used to identify an occurred fault and then as input of a supervisory system to generate alarm signals and to monitor the closed loop system's performance. The diagram of a fault tolerant control system considering fault diagnosis and supervision is represented in Fig. 1.

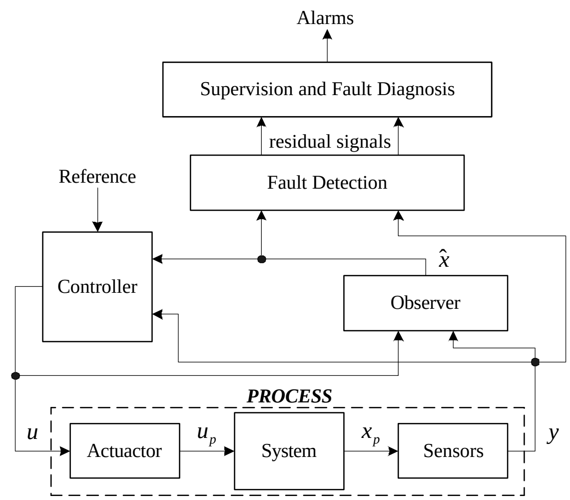

Fig. 1. Diagram of the fault tolerant control system considering fault diagnosis and supervision.

Concerning the control system, for the last few decades model-based predictive control (MPC) methodologies have increasingly been receiving the control community attention and recognition as a valuable approach in solving practical control problems. The MPC history can be traced back to the late 1970's with the Model Algorithm Control and the Dynamic Matrix Control techniques [5], where a linear description of the plant is considered. More recently, pushed by the non-linear nature of most industrial processes, some research efforts have been placed in the development of reliable non-linear model predictive control strategies (NMPC). The main drawback of "true" NMPC approaches is related to the online solution of a non-convex optimisation problem, since the convergence to a feasible/optimal solution and stability cannot be guaranteed in advanced, not to mention the unpredictable computation time that might be required.

Another issue concerning NMPC is that for many systems it might be difficult and rather expensive to come up with an enough accurate physical model of the plant required by MPC techniques. These limitations can mainly be attributed in most cases to the complexity of the underlying phenomena and/or to the lacking of some specific parameters. In these circumstances neural networks have proved to perform quite well in the identification of non-linear systems based on input-output data (see *e.g.* [6], [7] and [8]).

It is well known that neural networks are universal approximators [9]. However, it is also true that the accuracy of the neural predictor is extremely dependent on the quality of the training data set. In case of offline learning, this fact together with a bounded number of iterations and the implementation of regularization techniques in the learning stage inexorably leads to a model/plant mismatch, which is the expression of an impenetrable screen between the world of mathematical description and the real world. Thus, there will be steady state offset errors in the control system response. On the other hand, even in the case where neural network weights are adjusted online this situation might arise as a result of an adequate adaptation gain. To circumvent this effect on the control performance for instance in [10] it is suggested adding up to the system's step response an estimate of modelling errors. Alternatively, the incorporation in the control loop of an offset compensator only active in a narrow range from the set point is proposed in [11] and [12].

The overall control system obtained with these methodologies should improve the plant efficiency and the closed loop performance and robustness in presence of faults and disturbances. The fault-tolerant control system has been implemented in a Distributed Solar Collector field.

2. The fault Diagnosis module

Considering the model-based approach, a mathematical model is built and in a non-linear system case, a model linearisation, around several operating points, are performed. The deviations between the linear model and the real plant will be considered as uncertainties in the observer based detection module. For fault diagnosis purposes, the system is described including actuator and sensor faults, which are represented by additive signals as illustrated in Fig. 2.

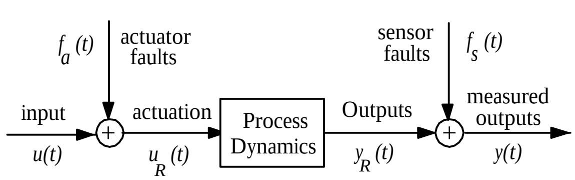

Fig. 2. System description with actuator and sensor faults.

The system dynamics can be described by the state space model (1):

$$\begin{aligned} \dot{x}(t)&=Ax(t)+Bu_R(t) \quad & y_R(t)&=Cx(t)+Du_R(t) \\ y(t)&=y_R(t)+f_s(t) \quad & u_R(t)&=u(t)+f_a(t) \end{aligned} \tag{1}$$

The residual signals, *r(t)*, generated by the fault detection filter are given by (2).

$$r(t) = K\begin{bmatrix} y(t) \\ \hat{x}(t) \end{bmatrix} \tag{2}$$

The consideration of a *fault diagnosis system* allows to detect, isolate and identify faults and to increase the robustness of the control system against faults by collecting and analysing information on system status using these residual signals and other information sources.

In this context, neural networks and fuzzy logic techniques (see e.g. [13]) could be combined with the more traditional use of robust observers, parity space methods and hypothesis-testing methodologies in order to enhance the prediction and decision making policies.

3. Extended MPC formulation

Model-based predictive control is a discrete-time technique where an explicit dynamic model of the plant is used to predict the system's outputs over a finite prediction horizon *P* when control actions are manipulated throughout a finite control horizon *M*. At time step k the optimiser computes on-line the optimal open-loop sequence of control actions such that the predicted outputs follow a pre-specified reference signal and taking into account possible hard and soft constraints. Only current control actions $u(k|k)$ are actually fed to the plant over the time interval $[k, k+1)$. Next, at time step $k+1$, the prediction and control horizons are shifted ahead by one step and a new optimisation problem is solved using the most recent measurements, and the control action fed to the plant in the previous time interval, $u(k|k)$.

Let the linearised discrete-time dynamics of a general non-linear system be described in the state-space form as follows:

$$\begin{aligned} \mathrm{x}(\mathrm{k}+1) &= \Phi\mathrm{x}(\mathrm{k}) + \Gamma\mathrm{u}(\mathrm{k}) + h \\ \mathrm{y}(\mathrm{k}) &= \Xi\mathrm{x}(\mathrm{k}) \end{aligned} \tag{3}$$

where $\Phi \in \Re^{n \times n}$, $\Gamma \in \Re^{n \times m}$ and $\Xi \in \Re^{p \times n}$ are, respectively, the state, input and output matrices; $x \in \Re^{n}$ is the state vector, $u \in \Re^{m}$ is the control vector and $y \in \Re^{p}$ the output vector; $h \in \Re^{n}$ is a constant vector related to the first term of the Taylor expansion, which is zero at any equilibrium point.

Considering a 2-norm for the cost functional and linear constraints on the inputs and outputs of the system and, additionally, bounds on the rate of change of control actions, the open-loop optimisation problem can be stated in the following way:

$$\min_{u} J = \min_{u} \left\{ \sum_{i=1}^{P} \| y(k+i \mid k) - r(k+i) \|_{Q_i}^{2} + \sum_{i=0}^{P-1} \| u(k+i \mid k) \|_{R_i}^{2} + \sum_{i=0}^{M-1} \| \Delta u(k+i \mid k) \|_{S_i}^{2} \right\} \quad (4)$$

subject to system dynamics (3) and to the following inequalities:

$$\begin{aligned} & y_{min} \le y(k+i|k) \le y_{max}, \quad i = 1, \dots, \ P, \quad k \ge 0 \\ & u_{min} \le u(k+i|k) \le u_{max}, \quad i = 0, \dots, \ P-1, \quad k \ge 0 \\ & |\Delta u(k+i|k)| \le \Delta u_{max}, \quad i = 0, \dots, \ M-1, \quad k \ge 0 \\ & |\Delta u(k+i|k)| = 0, \quad i = M, \dots, \ P-1, \quad k \ge 0 \end{aligned} \quad (5)$$

with $Q_i \in \Re^{p \times p}$, $R_i \in \Re^{m \times m}$, $S_i \in \Re^{m \times m}$, $\Delta u \in \Re^{m}$ is the control increment vector and $r \in \Re^{p}$ is the reference signal.

Given the convexity of the optimisation problem any particular solution is a global optimum and thus the open-loop optimal control problem can be restated as a quadratic programming problem (6) and (7).

$$\textit{minimise} \quad J(\Delta\tilde{u}) = h^{T} \Delta\tilde{u} + \frac{1}{2} \Delta\tilde{u}^{T} H \Delta\tilde{u} \quad (6)$$

$$\textit{Subject to} \quad A^{T} \Delta\tilde{u} \le b \quad (7)$$

where $A \in \Re^{mM \times (4mM + 2pP)}$, $b \in \Re^{(4mM+2pP)}$ and $\Delta\tilde{u} \in \Re^{mM}$ is the extended control increments over the control horizon.

In order to prevent from the effect of modelling errors that are responsible for static offsets, an offset compensator is incorporated in the control loop as depicted schematically in Fig. 3.

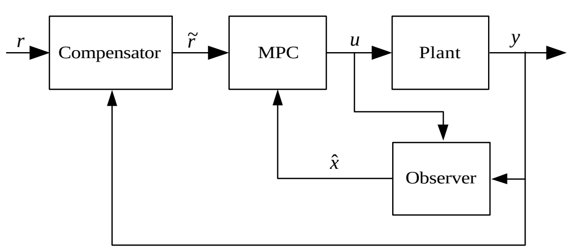

Fig. 3. Extended MPC Structure.

The filter works somehow as an integrator where the control error is previously weighted according to (8).

$$a(k) = \frac{k}{1 + [y(k) - r(k)]^{4}} \quad (8)$$

where k is an users defined constant.

Next, this summation is added up to the true reference signal before being supplied to the MPC structure. Since the weighting factor a is neglectable beyond a narrow range from the set point an effective manipulation of the reference signal provided to the optimizer only takes place in the vicinity of the set point, avoiding this way undesirables windup effects over the reference signal.

4. DSC Neural Modeling

The Acurex field modelling it carried out by means of a non-linear state space neural network. This structure comprises 3 layers of neurons, Fig. 4, where the input and the output layers incorporate one neuron, corresponding to the same number of inputs and outputs. The number of neurons in the hidden layer was chosen as 2 according to a trade-off between the generalisation performance and the training error.

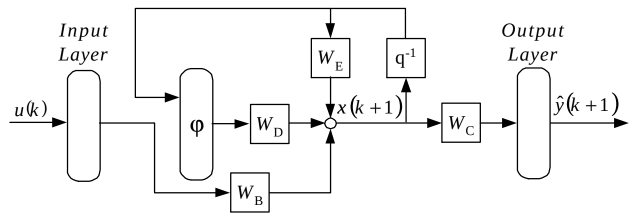

Fig. 4. Non-linear state-space neural network block diagram.

This neural network structure can be described in the state space form by the following equations, assuming j as a hyperbolic tangent function:

$$\begin{aligned} & x(k+1) = W_D \tanh(x(k)) + W_E x(k) + W_B u(k) \quad ; x(0) = x_0 \\ & \hat{y}(k) = W_C x(k) \end{aligned} \quad (9)$$

where $x(k) \in \Re^{Nn}$ is the network internal hyperstate, $\hat{y}(k) \in \Re^{No}$ is the network output, $u(k) \in \Re^{Ni}$ is the external input; Ni, Nn and No are, respectively, the number of neurons in the input layer, hidden layer and output layer.

The synaptic weights between neurons W_B, W_C, W_D and W_E are real-valued matrices with appropriate dimensions.

For the neural network training the present work follows a dual Kalman filter (DUKF) approach based on the unscented transformation [14]. In the DUKF approach both states and weights are computed simultaneously in two stages: *i*) in the time update one step-ahead predictions for the estimates are computed, while *ii*) in the measurement update a correction is provided to these estimates on the basis of current noisy measurement. The dual Kalman filter equations are given by:

Weights estimation

Time update:

$$\begin{aligned} & \Omega(k \mid k-1) = \Omega(k-1 \mid k-1) \\ & P_{ww}(k \mid k-1) = m^{-1} P_{ww}(k-1 \mid k-1) \\ & Z^{w}(k \mid k-1) = h(\hat{x}(k-1 \mid k-1), \Omega(k \mid k-1), k) \\ & \hat{z}_{w}(k \mid k-1) = \sum_{i=0}^{2Nw} \Gamma_i^{w} Z_i^{w}(k \mid k-1) \end{aligned} \quad (10)$$

Measurement update:

$$P_{nn}^{w}\left(k\mid k-1\right)=\sum_{i=0}^{2Nw}\left\{\Gamma_i^{w}\left[Z_i^{w}\left(k\mid k-1\right)-\hat{z}_w\left(k\mid k-1\right)\right]\right.$$
$$\left.\left[Z_i^{w}\left(k\mid k-1\right)-\hat{z}_w\left(k\mid k-1\right)\right]^{T}\right\}+R$$
$$P_{wz_w}\left(k\mid k-1\right)=\sum_{i=0}^{2Nw}\left\{\Gamma_i^{w}\left[\Omega_i\left(k\mid k-1\right)-\hat{w}\left(k\mid k-1\right)\right]\right.$$
$$\left.\left[Z_i^{w}\left(k\mid k-1\right)-\hat{z}\left(k\mid k-1\right)\right]^{T}\right\} \tag{11}$$
$$K^{w}\left(k\right)=P_{wz_w}\left(k\mid k-1\right)\left(P_{nn}^{w}\left(k\mid k-1\right)\right)^{-1}$$
$$\hat{w}\left(k\mid k\right)=\hat{w}\left(k\mid k-1\right)+K^{w}\left(k\right)\left[z\left(k\right)-\hat{z}\left(k\mid k-1\right)\right]$$
$$P_{ww}\left(k\mid k\right)=P_{ww}\left(k\mid k-1\right)-K^{w}\left(k\right)P_{nn}^{w}\left(k\mid k-1\right)K^{w}\left(k\right)^{T}$$

States estimation

Time update:

$$X\left(k\mid k-1\right)=f\left(X\left(k-1\mid k-1\right),u\left(k-1\mid k-1\right),w\left(k-1\mid k-1\right),k\right)$$
$$\hat{x}\left(k\mid k-1\right)=\sum_{i=0}^{2Nn}\Gamma_i^{x}X_i\left(k\mid k-1\right)$$
$$P_{xx}\left(k\mid k-1\right)=\sum_{i=0}^{2Nn}\Gamma_i^{x}\left[X_i\left(k\mid k-1\right)-\hat{x}\left(k\mid k-1\right)\right] \tag{12}$$
$$Z^{x}\left(k\mid k-1\right)=h\left(X\left(k\mid k-1\right),w\left(k-1\mid k-1\right),k\right)$$
$$\hat{z}_x\left(k\mid k-1\right)=\sum_{i=0}^{2Nn}\Gamma_i^{x}Z_i^{x}\left(k\mid k-1\right)$$

Measurement update:

$$P_{nn}^{x}\left(k\mid k-1\right)=\sum_{i=0}^{2Nn}\left\{\Gamma_i^{x}\left[Z_i^{x}\left(k\mid k-1\right)-\hat{z}_x\left(k\mid k-1\right)\right]\right.$$
$$\left.\left[Z_i^{x}\left(k\mid k-1\right)-\hat{z}_x\left(k\mid k-1\right)\right]^{T}\right\}+R$$
$$P_{xz_x}\left(k\mid k-1\right)=\sum_{i=0}^{2Nn}\left\{\Gamma_i^{x}\left[X\left(k\mid k-1\right)-\hat{x}\left(k\mid k-1\right)\right]\right.$$
$$\left.\left[Z_i^{x}\left(k\mid k-1\right)-\hat{z}_x\left(k\mid k-1\right)\right]^{T}\right\} \tag{13}$$
$$K^{x}\left(k\right)=P_{xz_x}\left(k\mid k-1\right)\left(P_{nn}^{x}\left(k\mid k-1\right)\right)^{-1}$$
$$\hat{x}\left(k\mid k\right)=\hat{x}\left(k\mid k-1\right)+K^{x}\left(k\right)\left[z\left(k\right)-\hat{z}\left(k\mid k-1\right)\right]$$
$$P_{xx}\left(k\mid k\right)=P_{xx}\left(k\mid k-1\right)-K^{x}\left(k\right)P_{nn}^{x}\left(k\mid k-1\right)K^{x}\left(k\right)^{T}$$

where m denotes the forgetting factor, Ω the sigma points matrix of *w*, Γ the corresponding weight vector, K the Kalman gain and X the sigma points matrix of *x*.

5. The solar thermal power plant

The distributed solar collector (DSC) field is part of the Plataforma Solar de Almería (PSA), Fig. 5. It is a center for testing thermal solar energy applications, located on the desert of Tabernas, in the south of Spain.

The DSC field consists of 480 parabolic trough collectors arranged in 20 rows aligned on a West-East axis and forming 10 independent loops. Every solar collector has a linear parabolic-shaped reflector that focuses the sun's beam radiation on a linear absorber tube located at the focus of the parabola. Each of the loops is 172 *m* long, with an active section of 142 *m*, while the reflective area of the mirrors is around 264.4 m^2.

The thermal oil is heated as it circulates through the absorber tube before entering the top of the storage tank. The colder inlet oil is extracted form the bottom of the tank. The thermal energy storage in the tank can be subsequently used to produce electrical energy in a conventional steam turbine/generator or in the solar desalination plant operation.

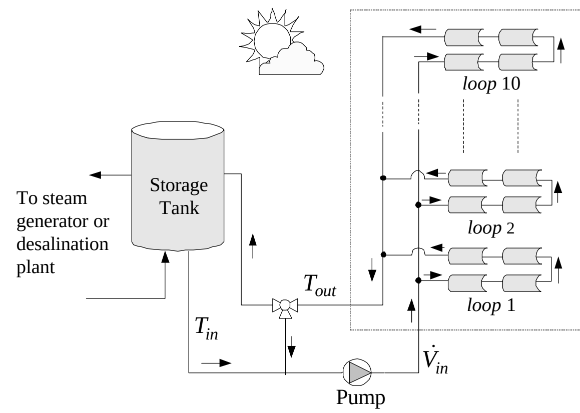

Fig. 5. Distributed solar collector field schematics.

6. Results

The main control prerequisite in a DSC field is to maintain the outlet oil temperature at a prescribed value by suitably manipulating the oil flow rate through the receivers. For this purpose, the proposed adaptive constrained non-linear MPC scheme with steady state offset compensation was tested on the Plataforma Solar de Almería Acurex field.

In all tests reported in this paper the sampling time was set to 15 seconds and the prediction horizon and the control horizon were chosen as $P=10$ and $M=1$ time steps.

To assess the robustness and fault tolerance properties of the proposed control scheme, some tests were carried out by injecting some specific mal-functions and disturbances, such as faults on sensors, on the actuator and on the system's parameters.

Test with an Adaptive MPC

In this test an adaptive neural model-based predictive control without steady offset compensation was used for controlling the DSC field (Fig. 6).

The main goal with this experiment was to gather information upon the performance of the control system without any offset compensation and to get a reliable term of comparison so as to enable assessing the performance of the steady-state offset compensation approach. The initial covariance matrices involved in the weights adaptation computations were chosen as $P_{xx}\left(0\right)=\mathbf{1}$ and $P_{ww}\left(0\right)=\mathrm{diag}(5\times10^{-3})$ and the forgetting factor m was set equal to 0.9986.

In figure 5 it is shown the outlet oil temperature (T_{out}), set point (T_{ref}), oil flow rate through each DSC loop (Q_{in}), the inlet oil temperature (T_{in}) and the solar radiation (Irr).

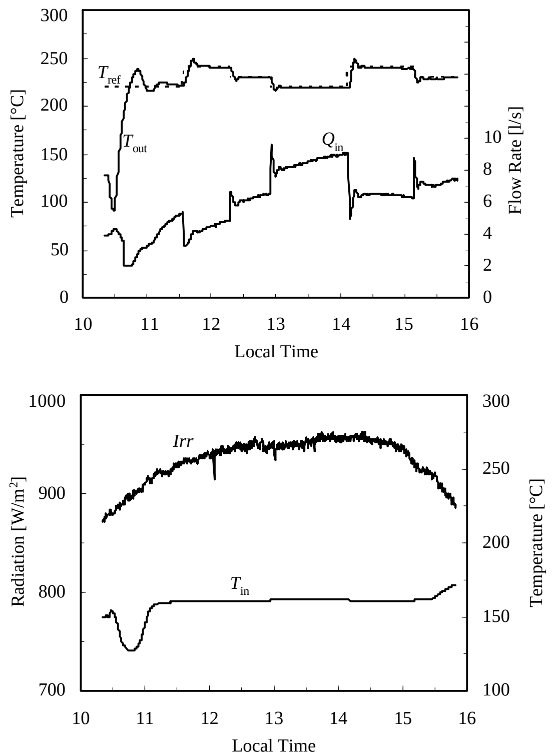

Fig. 6. ACUREX field test on the 17th July, 2002: Set point, outlet oil temperature and oil flow rate, solar radiation and inlet oil temperature.

As can be observed from the above plots, the adaptive MP control system provides upon the whole a very acceptable response of the outlet oil temperature.
Furthermore, as time goes on, as a result of an increasing model accuracy the steady state errors become gradually lower. However, in view of the fact the adaptation mechanism is rather smooth when the solar radiation starts falling after the noon the neural predictor becomes less accurate and so offset errors are once again observed. This new dynamics would be captured in case the test had not been stopped.

Test with an Adaptive MPC plus Offset Compensation

This control test was carried out using an adaptive neural model-based predictive control incorporating a steady offset compensator (Fig. 7). The initial covariance matrices for the DUKF were chosen as $P_{xx}(0) = \mathbf{1}$ and $P_{ww}(0) = \mathrm{diag}(2\times10^{-3})$. Further, the forgetting factor was set equal to 0.9987 and $k = 0.005$.
Figure 8 shows the outlet oil temperature (T_{out}), set point (T_{ref}), oil flow rate through each DSC loop (Q_{in}), the inlet oil temperature (T_{in}) and the solar radiation (Irr).
As can be observed from the above plots, this MPC scheme is able to drive the outlet oil temperature to the desired value even in the initial control stage where it is expected significant modelling errors. However, the price to pay is a more oscillating control system time response.

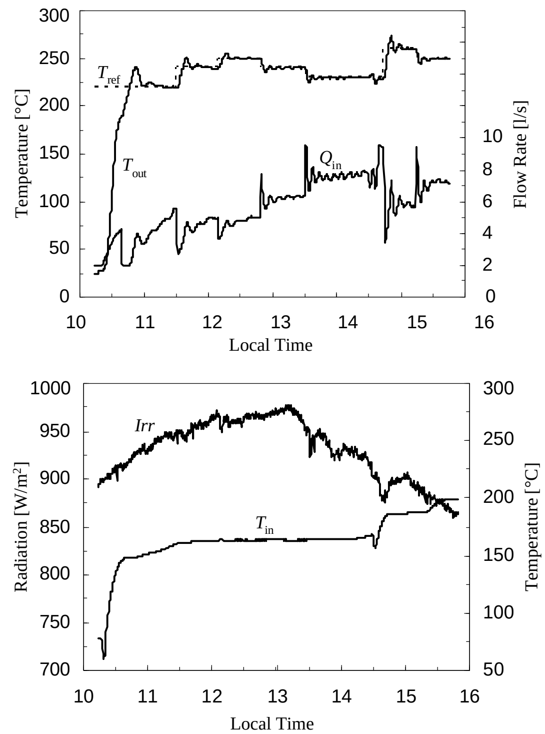

Fig. 7. ACUREX field test on the 23th July, 2002: Set point, outlet oil temperature and oil flow rate, solar radiation and inlet oil temperature.

Test with an Adaptive MPC plus Offset Compensation in the Presence of Faults

This control test was carried out using an adaptive neural model-based predictive control incorporating a steady offset compensator, in the presence of some faults (Fig. 8). At 13:03 and at 13:07 the loops 6 and 4 were, respectively, disconnected, and at 13:53, these flow rates were re-established. From 14:36 to 15:03 a perturbation was introduced on the inlet temperature with maximum amplitude around 50ºC. At 15:10 an offset of +10ºC was added up to the outlet oil temperature for 16 minutes. At 15:37 an inlet oil temperature offset of +10ºC was injected for 9 minutes.
Figure 8 shows the outlet oil temperature (T_{out}), set point (T_{ref}), oil flow rate through each DSC loop (Q_{in}), the inlet oil temperature (T_{in}) and the solar radiation (Irr).
As can be observed from the above plots, the MPC scheme presents not only a quite well performance in driving the outlet oil temperature to the desired value but also a significant robustness considering the introduced faults. Actually, with this controller, the faults in system parameters (disconnection of loops) have almost no effects upon its behaviour. Regarding the perturbation on the inlet oil temperature it is noticed that it has a significant impact on the system’s response. Nevertheless, the controller was effectively able to deal with this type of disturbances without a significantly deterioration of the overall performance.

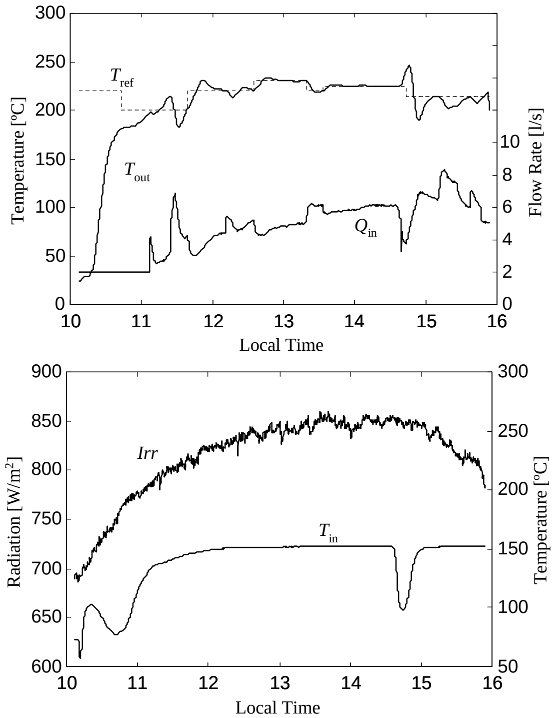

Fig. 8. ACUREX field test on the 31st July, 2002: Set point, outlet oil temperature and oil flow rate, solar radiation and inlet oil temperature.

For the two faults on the sensors, one must infer that improvements should be considered by incorporating a fault diagnosis module and a supervisory system in order to detect, identify and accommodate these types of faults.

7. Conclusion

In this work an adaptive constrained model-based predictive control scheme with steady state offset compensation was tested on a Distributed Solar Collector field at the Plataforma Solar de Almería. This strategy was compared with an adaptive MPC strategy without incorporating an offset compensator so as to asses the overall control system performance.

Results show the feasibility of the proposed control scheme and its robustness to the tested faults.

The results obtained with the tests carried out on the DSC field, are the input of the fault diagnosis module within a supervision framework. It is expected that the proposed framework, will enhance the overall control system performance, fault tolerance and robustness.

8. Acknowledgement

This work was partially supported by POSI–*Programa Operacional da Sociedade de Informação* of Portuguese Fundação para a Ciência e Tecnologia and by the European Union's FEDER and PRAXIS XXI ALCINE Projects. The experiments were carried under the support of the "Improving Human Potential" programme of EU-DGXII. The authors wish to express their gratitude to the PSA staff.

References

[1] A. Ichtev, J. Hellendoorn, R. Babuska and R. Mollov, Fault-Tolerant Model-Based Predictive Control Using Multiple Takagi-Sugeno Fuzzy Models, *FUZZ-IEEE'02. Proceedings of the 2002 IEEE International Conference on Fuzzy Systems*, 1, 2002, 346 –351.

[2] P. M. Frank and X. Ding, Survey of robust residual generation and evaluation methods in observer-based fault detection systems. *Journal of Process Control*, 7(6), *1997*, 403-424.

[3] J. Chen and R. J. Patton, *Robust Model-Based Fault Diagnosis for Dynamic Systems*. Kluwer Academic Publishers, 1999.

[4] R. S. Mangoubi and A. M. Edelmayer, Model Based Fault Detection: The Optimal Past, the Robust Present and a Few Thoughts on the Future, *Proceedings of the IFAC Symposium SAFEPROCESS'2000*, Budapest, Hungary, 2000, 64-75.

[5] C. Garcia, D. Prett and M. Morari, Model predictive control: Theory and practice – a survey, *Automatica*, 25(3), 1989, 335-348.

[6] I. Rivals and L. Personnaz, Black-box modelling with state-space networks, *Neural Adaptive Control Technology*, (R. Zbikowski and J. Hunt eds., World Scientific, 1996), 237-264.

[7] T. Yamada and T. Yabuta, Dynamic System Identification Using Neural Networks, *IEEE Trans. On Systems, Man and Cybernetics*, 23(1), 1993, 204-211.

[8] K. Narendra and K. Parthasarathy, Identification and Control of Dynamical Systems Using Neural Networks, *IEEE Trans. On Neural Networks*, 1(1), 1990, 4-27.

[9] K. Hornik, M. Stinchcombe and H. White, Multilayer Feedforward Networks are Universal Approximators, *Neural Networks*, 2, 1989, 359-366.

[10] A. Draeger, S. Engell and H. Ranke, Model predictive control using neural networks, *IEEE Control Systems Magazine*, 15(5), 1995, 61-66.

[11] P. Gil, J. Henriques, A. Dourado and H. Duarte-Ramos, Constrained Neural Model Predictive Control with Guaranteed Free Offset, *Proc. 2000 IEEE Int. Conf. on Industrial Electronics, Control and Implementation – IEECON*, Nagoya, Japan, 2000, 1991-1996.

[12] P. Gil, J. Henriques, P. Carvalho, H. Duarte-Ramos and A. Dourado, Adaptive Neural Model-Based Predictive Control of a Solar Power Plant, *IEEE International Joint Conference on Neural Networks*, Honolulu, HI-USA, 2002.

[13] X. Zhang, M. Polycarpou, and T. Parisini, A Robust Detection and Isolation Scheme for Abrupt and Incipient Faults in Nonlinear Systems, *IEEE Transactions on Automatic Control*, 47(4), 2002, 576-593.

[14] S. Julier, J. Uhlmann and F. Durrant-Whyte, A New Method for the Nonlinear Transformation of Means and Covariances in Filters and Estimators, *IEEE Trans. Aut. Control*, 45, 2000, 477-482.